An advanced dielectric continuum approach for treating solvation effects: Time correlation functions. I. Local treatment

M. V. Basilevsky, D. F. Parsons, and M. V. Vener
Karpov Institute of Physical Chemistry, ul. Vorontsovo Pole 10, Moscow 103064, Russia

(Received 16 January 1997; accepted 7 October 1997)

A local continuum solvation theory, exactly treating electrostatic matching conditions on the boundary of a cavity occupied by a solute particle, is extended to cover time-dependent solvation phenomena. The corresponding integral equation is solved with a complex-valued frequency-dependent dielectric function $\varepsilon(\omega)$, resulting in a complex-valued ω-dependent reaction field. The inverse Fourier transform then produces the real-valued solvation energy, presented in the form of a time correlation function (TCF). We applied this technique to describe the solvation TCF for a benzophenone anion in Debye (acetonitrile) and two-mode Debye (dimethylformamide) solvents. For the Debye solvent the TCF is described by two exponential components, for the two-mode Debye solvent, by three. The overall dynamics in each case is longer than that given by the simple continuum model. We also consider a steady-state kinetic regime and the corresponding rate constant for adiabatic electron-transfer reactions. Here the boundary effect introduced within a frequency-dependent theory generates only a small effect in comparison with calculations made within the static continuum model. © *1998 American Institute of Physics.*
[S0021-9606(98)50403-5]

I. INTRODUCTION

In the present work we consider time-dependent solvation phenomena in polar media in terms of a refined continuum medium model. The corresponding experimental data[1–7] include both observations of time-resolved fluorescence spectra (Stokes shifts) in polar solvents and the more traditional measurements of electron transfer (ET) kinetics. For the last decade several theoretical approaches in this field have been tested. They include direct MD simulations,[8–18] the computations of spatial pair correlation functions based on interaction site models (i.e., statistical equilibrium theories), extended to cover time dependence,[19–22] dynamical developments of the mean spherical approximation (MSA)[23–25] a nonlocal continuum theory,[26] and other semianalytical treatments.[7,27–35] All these approaches represent microscopic molecular solvent theories at various levels of sophistication. It is commonplace to claim that continuum medium models are incapable of adequately treating solvation dynamics.[1–6,24,27,30,34] The basic motivation is that, for Debye solvents, the continuum theory predicts monoexponential kinetics for solvent relaxation from an instantaneous change in the solute charge distribution in ionic solutes. This contradicts both experiment and the abovementioned microscopic treatments.

The objective of our work is to demonstrate that reasonable modifications of the conventional continuum solvent model enable one to overcome this deficiency. The thus improved continuum theories are able to qualitatively monitor the same picture of polar solvent dynamics as do molecular theories. Then, by properly adjusting the model parameters (a feature which is common for both molecular and continuum models), experimental dependencies can be well reproduced. With this background the following important (usually disregarded) advantage of continuum treatments becomes decisive: Being combined with modern quantum-chemical calculations they allow a precise description of electronic structure and charge distributions in chemically nontrivial solute species, whereas all recent molecular treatments invoke crude solute models and concentrate on a description of the details of solvent structure.

Two types of effects must be incorporated in a time-dependent continuum theory so that may become satisfactory for studying solvation dynamics. We shall refer to the first one as the ''boundary effect'' and the second one as the ''effect of solvent structure.'' The first effect can be formulated within the Born-Kirkwood-Onsager (BKO) solvation model. This static treatment mimics equilibrium solvation as result of purely electrostatic interactions between a solute charge density, contained in a cavity, and the solvent polarization induced by this charge in the continuum medium outside the cavity. With a single medium parameter, the static dielectric constant ε_0, the BKO model may be successfully applied for complicated solutes of arbitrary size and shape.[36] The electrostatic problem to be solved is the Poisson equation with relevant matching conditions for its solution on the cavity boundary. Efficient techniques for numerically calculating this solution are well developed for the static case.[36] Such an approach has also been extended to treat, still at a static level, nonequilibrium solvation effects[37–40] and has been used in computing free energy surfaces and profiles.[39,41–44] When proceeding to a dynamical treatment, the exact electrostatic boundary conditions have always been neglected because of technical difficultes, although a formal theory matching time-dependent electrostatic fields on the boundary has been reported.[37] So, the development of a dynamical BKO theory, for correctly treating the boundary conditions (which till now has been readily available only at a static level), is necessary.

This article is copyrighted as indicated in the article. Reuse of AIP content is subject to the terms at: http://scitation.aip.org/termsconditions. Downloaded to IP: 134.115.2.116 On: Fri, 17 Jul 2015 07:43:17

The second effect appears due to an incorporation of elements of solvent structure in the continuum model. This can be done in the framework of nonlocal electrostatics.[45–48] The time-dependent nonlocal theory of Stokes shifts has been reported.[26] It was based on an approach[45–48] where excluded volume effects were not explicitly considered. Attempts of an accurate treatment of cavity effects within a static nonlocal theory have been announced.[49–51] Their dynamical development is in order.

It must be emphasized that a nonlocal approach is in practice available only for spherically symmetrical objects. For such cases the BKO boundary effect vanishes. Indeed, for a spherically symmetric ion the BKO model comprises a simple Born treatment which, being extended to the description of time resolved Stokes shifts in Debye solvents, is well known to yield (in conflict with experiment) a single-exponential kinetic evolution with a characteristic time τ_L, the longitudinal relaxation period. This means that at the present technical level (spherically symmetrical solutes within a nonlocal electrostatic treatment) the two abovementioned effects appear as mutually complementary ones: The first brings an influence of boundary matching conditions for nonspherical cavities and solute charge distributions, the second introduces elements of internal solvent structure in describing the solvation of simplified solutes reduced to spherically symmetric models.

An important simplification inherent to the linear response approach is that the relevant dynamic dependencies can be deduced as a straightforward extrapolation of equilibrium equations of the corresponding static theory. This fact was emphasized and utilized independently for application to nonstationary kinetics with stepwise initial conditions (in the context of the MSA treatment of time-dependent Stokes shifts[23]) and also for deriving the steady-state KGH kinetics of ET (in the framework of a simple continuum ET theory[52]). Later this idea was widely exploited.[24,25,27,34,35] Its most recent applications[27,34,35] have some features in common with the present dynamical treatment. In their practice these theories focus on the account of the first of two effects, classified above as a local BKO boundary effect. The present article also reports only BKO calculations. The novel methodical element in an incorporation of the time (or frequency) dependent linear-response methodology in a standard numerical BKO SCRF procedure.[36] This makes practically available the computations of time-correlation functions (TCFs) for real chemically interesting objects of complicated shape with their charge distributions found in a direct quantum-chemical treatment. The extention of this technique to treat the second effect (the solvent molecular structure) in the frame of a nonlocal theory will be a subject of a future publication.

The kinetic regimes we are going to investigate cover two types of solvation dynamical experiments. First, we study the kinetics of medium relaxation in the vicinity of an instantaneously created ion in a polar solvent. The other regime corresponds to a steady-state kinetics typical for ET rate measurements, in which the role of initial conditions is suppressed. This case is conventionally treated in terms of the Kramers-Grote-Hynes (KGH) theory[53] which is also applied in our work. The two types of TCFs needed to describe these two experimental situations are derived within the framework of a unified linear response picture for describing charge redistribution within the chemical objects under examination. The logical structure of this approach, common for both local and nonlocal background theories, is exposed in Sections III, V, VI. Most immediate applications are considered in Sections V and VI at the local BKO level.

II. EQUILIBRIUM SOLVATION EFFECTS IN A DIELECTRIC CONTINUUM REPRESENTATION

Let us provide a continuum calculation of the solvation energy as an example. Only longitudinal fields are considered. The basic linear response relation connecting the solute charge density $\rho(r)$ (a ''force'') with the induced medium reaction field $\Phi(r)$ (a ''response'') reads

$$\Phi(r)=\hat{K}\rho(r), \tag{2.1}$$

where $\hat{K}$ is a linear integral operator with kernel $K(r,r')$; the corresponding explicit representation of this operator relation is

$$\Phi(r)=\int d^3r'K(r,r')\rho(r'). \tag{2.2}$$

We shall consider $\hat{K}$ as a generalized susceptibility operator, $K(r,r')$ is the corresponding nonlocal susceptibility kernel. In many typical cases an explicit description (2.2) of the operator $\hat{K}$ is unavailable in practice; an alternative is provided by a linear computational algorithm which numerically represents this relation. For instance, in the BKO solvation model[36] we treat the solvent as a dielectric continuum with dielectric constant ε_0 and susceptibility χ_0

$$\chi_0=\frac{1}{4\pi}(\varepsilon_0-1). \tag{2.3}$$

This continuum fills the whole space outside the cavity occupied by the solute. With the cavity surface denoted by S we use the notation V_i and V_e for the volumes inside and outside of S, respectively. In the BKO theory the solute charge $\rho(r)$ induces a charge density $\sigma(r)$ on the surface S and the reaction field $\Phi(r)$ is defined as its potential

$$\Phi(r)=\int_S d^2r'\,\frac{\sigma(r')}{|r-r'|}. \tag{2.4}$$

Given a charge distribution $\rho(r)$, the surface charge $\sigma(r)$ is found as a solution to a linear integral equation containing $\rho(r)$. The symbolic relation (2.1) then means: Solve this integral equation and apply formula (2.4).

Another example of an algorithmic application of the linear relation (2.1) is a nonlocal dielectric continuum theory with a cavity.[50,51] Here the field $\Phi(r)$ is created by a combination of a surface charge $\sigma(r)$ and a charge distribution $g(r)$ which is induced in the bulk medium outside the cavity

$$\Phi(r)=\int_{V_e} d^3r'\,\frac{g(r')}{|r-r'|};\quad g(r)=0(r\in V_i). \tag{2.5}$$

This article is copyrighted as indicated in the article. Reuse of AIP content is subject to the terms at: http://scitation.aip.org/termsconditions. Downloaded to IP: 134.115.2.116 On: Fri, 17 Jul 2015 07:43:17

The input medium characteristic is now the dielectric susceptibility kernel $\chi(r,r')$, a nonlocal counterpart of the static susceptibility χ_0 (2.3). It is defined as

$$\chi(r,r')=\begin{cases}\chi(|r-r'|) & r,r'\in V_e\\ 0 \quad r \text{ or } r'\in V_i\end{cases}. \tag{2.6}$$

The surface charge $\sigma(r)$ and external charge density $g(r)$ are found as a solution to the corresponding integral equation containing $\chi(|r-r'|)$. Usually a parametrization of this quantity is performed in terms of its Fourier transform $\chi(k)$, we then obtain $\chi(|r-r'|)$ as an inverse Fourier transform. The corresponding computation at the present moment is only available[50,51] for spherically symmetrical solutes with $\chi(k)$ given as a sum of Lorentzian modes.[26,45,48]

The equilibrium solvation energy in continuum theory has the same expression for the both models discussed above

$$U_0=\frac{1}{2}\int d^3r\rho(r)\Phi(r), \tag{2.7}$$

where the integration is actually performed only over the internal volume V_i because of an obligatory constraint imposed on the solute charge density

$$\rho(r)=0(r\in V_e). \tag{2.8}$$

Before proceeding to a discussion of the time dependence of the solvation energy we have to eliminate its inertialess high-frequency component U_∞ which is specially calculated by the same scheme described above

$$\begin{aligned}&\Phi_\infty(r)=\hat{K}_\infty\rho(r),\\ &U_\infty=\frac{1}{2}\int d^3r\rho(r)\Phi_\infty(r).\end{aligned} \tag{2.9}$$

The operator $\hat{K}_\infty$ differs from operator $\hat{K}$ of (2.1) only by changing the static dielectric constant ε_0 for the high-frequency constant ε_∞ in the integral equation for the surface charge density. We assume that the high-frequency permittivity kernel $\chi_\infty(|r-r'|)$ is local

$$\chi_\infty(k)=\chi_\infty=\frac{1}{4\pi}(\varepsilon_\infty-1). \tag{2.10}$$

In this instance the procedure (2.9) becomes common for both BKO and nonlocal theories.

III. THE DYNAMICAL LINEAR RESPONSE APPROACH WITHIN A DIELECTRIC CONTINUUM REPRESENTATION

The dynamical theory is based on the linear response relation

$$\Phi(r,\omega)=\hat{T}(\omega)\rho(r|\omega) \tag{3.1}$$

which extends the static equation (2.1) over the whole spectrum of frequency ω. The frequency-dependent complex-valued operator $\hat{T}(\omega)$ reduces to $\hat{K}$ in the static case

$$\hat{T}(\omega=0)=\hat{K}. \tag{3.2}$$

A simple example of an application of the basic relation (3.1) is a linear response estimation of the time-dependent solvation energy (more precisely its interaction component) defined as

$$U_S(t)=\int d^3r\rho_0\Phi(t). \tag{3.3}$$

(The r-dependence of relevant field quantities is suppressed for brevity here and in the forthcoming text unless this leads to confusion.) In Eq. (3.3) $\Phi(t)$ is a time-dependent reaction field describing the relaxation of an instantaneously created fluctuation $\Phi(t=0)$ to an equilibrium value Φ_0 given by Eq. (2.1)

$$\Phi_0=\hat{K}\rho_0. \tag{3.4}$$

The dynamic quantity of main interest, the field $\Phi(t)$, is obtained in terms of the basic equation (3.1) via an inverse Fourier transform.

An explicit expression for the dynamical operator $\hat{T}(\omega)$ is hardly available but we can construct its matrix representation. The method for doing this follows earlier reasoning applied in the static case.[37–39] We introduce a basis set of relevant charge distributions $\rho_{ab}(r)$ which is implied to be sufficient for describing the evolution of the solute charge density $\rho(r|\omega)$

$$\rho(r|\omega)=\sum_{ab}\rho_{ab}(r)m_{ab}(\omega)=\langle\langle\overline{\rho|}m(\omega)\rangle\rangle, \tag{3.5}$$

where $m_{ab}(\omega)$ are expansion coefficients determined by the conditions of an experiment. We have collected here the basis densities in a row-vector $\langle\langle\overline{\rho|}$

$$\langle\langle\overline{\rho|}=(\rho_{11},\rho_{22},\ldots,\rho_{12},\ldots) \tag{3.6}$$

and the expansion coefficients in a column-vector $|m(\omega)\rangle\rangle$

$$|m(\omega)\rangle\rangle=\begin{pmatrix}m_{11}(\omega)\\ m_{22}(\omega)\\ \vdots\\ m_{12}(\omega)\\ \vdots\end{pmatrix}. \tag{3.7}$$

(Double indices (ab) are used rather than single ones because in practice the basis functions ρ_{ab} are generated in terms of the CI theory[37–39] as elements of a transition density matrix with a special convention choosing cross-indices with $a\neq b$.) The corresponding set of basis reaction fields $\Phi_{ab}(r)$ is constructed in terms of the static (equilibrium) equation (2.1). We collect them in the row-vector

$$\langle\langle\overline{\Phi|}=\hat{K}\langle\langle\overline{\rho|}. \tag{3.8}$$

Thereby an expansion of the reaction field $\Phi(r|\omega)$ which is analogous to Eq. (3.5) is given by

$$\begin{aligned}\Phi(r|\omega)=\sum_{ab}\Phi_{ab}(r)n_{ab}(\omega)&=\langle\langle\overline{\Phi|}n(\omega)\rangle\rangle\\ &=\hat{K}\langle\langle\overline{\rho|}n(\omega)\rangle\rangle,\end{aligned} \tag{3.9}$$

where $|n(\omega)\rangle\rangle$ is a column-vector of expansion coefficients $n_{ab}(\omega)$.

This article is copyrighted as indicated in the article. Reuse of AIP content is subject to the terms at: http://scitation.aip.org/termsconditions. Downloaded to IP: 134.115.2.116 On: Fri, 17 Jul 2015 07:43:17

We construct now a set of medium dynamic variables Y_{ab} by defining their Fourier transforms as

$$Y_{ab}(\omega)=\int d^3r\rho_{ab}(r)\Phi(r|\omega) \tag{3.10}$$

and collecting them in a column-vector

$$|Y(\omega)\rangle\rangle=\int d^3r|\overline{\rho}\rangle\rangle\Phi(r|\omega), \tag{3.11}$$

where $|\overline{\rho}\rangle\rangle$ is the transpose of $\langle\langle\overline{\rho}|$, Eq. (3.6). By combining Eqs. (3.9) and (3.11) we obtain

$$|Y(\omega)\rangle\rangle=T_0|n(\omega)\rangle\rangle \tag{3.12}$$

with matrix T_0 defined as

$$T_0=\int d^3r|\overline{\rho}\rangle\rangle\hat{K}\langle\langle\overline{\rho}|, \tag{3.13}$$

which is known as the static reorganization matrix[39] (a ''minus'' sign has been omitted, contrary to the notation of Ref. 39). We can also define the dynamic reorganization matrix $T(\omega)$

$$T(\omega)=\int d^3r|\overline{\rho}\rangle\rangle\hat{T}(\omega)\langle\langle\overline{\rho}|. \tag{3.14}$$

Now, if one rewrites the linear response relation (3.1) as

$$\Phi(\omega)=\hat{T}(\omega)\langle\langle\overline{\rho}|m(\omega)\rangle\rangle, \tag{3.15}$$

then multiplies this on the left by $|\overline{\rho}\rangle\rangle$ and integrates, the result becomes

$$|Y(\omega)\rangle\rangle=T(\omega)|m(\omega)\rangle\rangle. \tag{3.16}$$

The relationship between the expansion coefficients is also established with the aid of Eq. (3.12)

$$|n(\omega)\rangle\rangle=T_0^{-1}T(\omega)|m(\omega)\rangle\rangle. \tag{3.17}$$

The direct utility of these formal relations may be recognized by noting that the time-dependent solvation energy (Eq. (3.3)) can be expressed as

$$U_S(t)-U_S(t=\infty)=Y_{11}(t)-Y_{11}(\omega=0). \tag{3.18}$$

Here we have assumed $\rho_0=\rho_{11}$ and have defined $Y_{ab}(t)$ as the inverse Fourier transform of $Y_{ab}(\omega)$. The function $\Phi(\omega)$ is defined in terms of expansion coefficients $m_{ab}(\omega)$ according to Eq. (3.15). If we take

$$m_{ab}(\omega)=\delta_{ab,11}\left[\lim_{\varepsilon\to+0}\frac{1}{i\omega-\varepsilon}\right] \tag{3.19}$$

(where the quantity in square brackets is the Fourier transform of the Heaviside step function $\Theta(t)$), this corresponds to

$$\rho(t)=\rho_{11}\Theta(t),$$

$$\Phi(t)=\int_{-\infty}^{t}d\tau\hat{T}(t-\tau)\rho(\tau)=\left[\int_0^t d\tau\hat{T}(\tau)\right]\rho_{11}, \tag{3.20}$$

$$U_S(t)-U_S(t=\infty)=\int_0^t d\tau T_{11,11}(\tau)-(T_0)_{11,11},$$

where $T_{11,11}(\tau)$ is the inverse Fourier transform of $T_{11,11}(\omega)$. The operator $\hat{T}(\tau)$ acts on functions of r and is the inverse Fourier transform of $\hat{T}(\omega)$.

Such a representation of $\Phi(t)$ corresponds to a model experimental situation[1–7] when the charge distribution ρ_{11} is instantaneously created at $t=0$. Henceforth we work with a dimensionless quantity, the solvation TCF

$$C(t)=\frac{U_S(t)-U_S(\infty)}{U_S(0)-U_S(\infty)}. \tag{3.21}$$

It should also be commented that linear response relations like (3.1), (3.16) represent properties of statistical averages of dynamical variables like $\Phi(t)$ or $Y(t)$. Strictly speaking, it is these averages $\langle\Phi(t)\rangle$ or $\langle\Phi(\omega)\rangle$ and $\langle Y(t)\rangle$ or $\langle Y(\omega)\rangle$ which enter the equations of this Section. Their fluctuations are introduced in Section VI in terms of the generalized Langevin description. At this (true microscopic) level of description the time-dependent solvation energy (3.18) is governed by the TCF

$$J(t)=\langle Y_{11}(t)Y_{11}(0)\rangle. \tag{3.22}$$

We show in Appendix A that this refined treatment gives the same result as Eqs. (3.18), (3.20).

IV. THE METHODOLOGY OF DYNAMICAL CALCULATIONS

We need now an explicit prescription for evaluating matrix $T(\omega)$ (Eq. (3.14)) in order to proceed to practical calculations. This prescription is given by the notion[37,52] that within a linear dielectric continuum treatment based on phenomenological Maxwell equations, the dynamical equations relating the Fourier transforms of time-dependent field quantities can be deduced from similar static equations for the corresponding equilibrium quantities. (A similar ansatz also works in the case of the MSA.[23]) The procedure needed is a simple change of relevant static susceptibilities (the linear response coefficients) for their dynamical counterparts, which are complex-valued functions of frequency ω. Thereby, the dynamic operator $\hat{T}(\omega)$ (3.1) is obtained from the static susceptibility operator $\hat{K}$ (2.1) by simply changing the static quantities ε_0 (the BKO theory) or $\chi(k)$ (the nonlocal theory) for the functions

$$\varepsilon(\omega)=\varepsilon_1(\omega)+i\varepsilon_2(\omega) \quad \text{(the BKO theory)}, \tag{4.1}$$

$$\chi(k,\omega)=\chi_1(k,\omega)+i\chi_2(k,\omega) \quad \text{(the nonlocal theory)}. \tag{4.2}$$

This actually means that we solve the same static integral equations (one for the BKO case, another for the nonlocal case) with the complex-valued functions (4.1) or (4.2) substituted for their static counterparts (see Appendix B for technical details). As a result one obtains intermediate auxiliary complex-valued charge densities

$$\sigma(\omega)=\sigma_1(\omega)+i\sigma_2(\omega) \quad \text{(the BKO and nonlocal theories)}, \tag{4.3}$$

This article is copyrighted as indicated in the article. Reuse of AIP content is subject to the terms at: http://scitation.aip.org/termsconditions. Downloaded to IP: 134.115.2.116 On: Fri, 17 Jul 2015 07:43:17

$$g(\omega)=g_1(\omega)+ig_2(\omega) \quad \text{(the nonlocal theory)}. \tag{4.4}$$

The complex-valued response fields

$$\Phi(\omega)=\Phi_1(\omega)+i\Phi_2(\omega) \tag{4.5}$$

are obtained in terms of the same equations (2.4), (2.5). Finally, the medium variables $Y_{ab}(\omega)$ are available from Eq. (3.16). Matrix $T(\omega)$ in this equation is calculated according to Eq. (3.14) with relevant pairs of basis charge densities. So, in order to calculate $T_{ab,cd}$, we first calculate the field $\Phi_{cd}(\omega)=\hat{T}(\omega)\rho_{cd}$ as described by Eqs. (4.1)–(4.5) and then evaluate its integral (3.14) with ρ_{ab}. In practice it is expedient to work with the quantities concerned with the inertial components of corresponding fields. The separation of the noninertial component is performed by the obvious relations

$$\begin{aligned} &T_{in}(\omega)=T(\omega)-T(\omega\to\infty),\\ &\Phi_{in}(\omega)=\Phi(\omega)-\Phi(\omega\to\infty),\\ &|Y_{in}(\omega)\rangle\rangle=T_{in}(\omega)|m(\omega)\rangle\rangle. \end{aligned} \tag{4.6}$$

Note that the calculation of matrix $T(\omega\to\infty)$ corresponds to a static BKO calculation with ε_∞ taken for the dielectric constant (as discussed at the end of Section II) because, at the operator level,

$$\hat{T}(\omega\to\infty)=\hat{K}_\infty. \tag{4.7}$$

For the time-dependent solvation energy (3.20) we obtain, by subtracting the constant inertialess part,

$$U_S(t)-U_S(t=\infty)=\int_0^t d\tau[T_{in}(\tau)]_{11,11}-[T_{0,in}]_{11,11}. \tag{4.8}$$

For the experimental situation as modelled by Eqs. (3.19), (3.20), the response field $\Phi_{in}(t)$ vanishes at $t=0$.

In this context, the frequency-dependent reorganization matrix

$$T_{in}(\omega)=[T_{in}(\omega)]_1+i[T_{in}(\omega)]_2 \tag{4.9}$$

becomes a key quantity in a dynamical treatment. In the third line of Eq. (4.6) the quantities $|m(\omega)\rangle\rangle$ and $|Y_{in}(\omega)\rangle\rangle$ may be interpreted as vectors of ''forces'' and ''responses,'' respectively. Hence, the matrix elements

$$[T_{in}(\omega)]_{ab,cd} \tag{4.10}$$

are complex-valued susceptibilities (response functions) obeying general theorems of the linear response theory. These special properties are useful in applications. For instance, TCFs of medium variables $[Y_{in}]_{ab}$ are readily obtained from quantities (4.10) by applying the fluctuation-dissipation theorem (FDT).

The solute charge distribution remains real in the present treatment. This is sufficient within a purely linear response approach. Nonlinear effects of solute polarization by the solvent reaction field Φ appear when the solute charge distribution $\rho(r)$ is calculated as a functional of $\Phi(r)$: $\rho=\rho[\Phi]$. Thereby, ρ would necessarily become complex-valued in a nonlinear treatment (cf. the SCRF method[36]) based on the present approach with complex-valued Φ. Such effects could be incorporated in our scheme, but this sophistication was not included in the equations of Appendix B where ρ is considered as a fixed real quantity.

V. BKO CALCULATIONS AND THEIR RESULTS

Our test calculations were performed with a benzophenone anion as the solute. This seems to be the only polyatomic ion for which solvation dynamics in the ground electronic state in *n*-butanol has been experimentally studied.[54,55] Its geometry was taken to be the same as that of the neutral molecule found by standard optimization procedures using the PM3 method. The value of the dihedral angle between the planes of benzene rings was taken to be 30°. Its charge distribution was calculated within a standard quantum-chemical BKO SCRF procedure basing on a semiempirical PM3 scheme. We studied several polar solvents, which are characterised by different types of dielectric dispersion. The quantity we calculated and investigated was the diagonal element of the reorganization matrix $T_{in}(\omega)$ for the lowest electronic state of the benzophenone anion. For brevity we denote it as

$$[T_{in}(\omega)]_{11,11}=E(\omega)=E_1(\omega)+iE_2(\omega). \tag{5.1}$$

It plays the role of susceptibility in the linear response relation (4.6) and henceforth will be called the ''response function.'' Thus, the real functions $E_1(\omega)$ and $E_2(\omega)$ obey standard symmetry constraints[56]

$$\begin{aligned} &E_1(\omega)=E_1(-\omega),\\ &E_2(\omega)=-E_2(-\omega), \end{aligned} \tag{5.2}$$

which were well reproduced in our test calculations. Other technical details are given in Appendix B.

In the framework of a simple continuum medium model[52,57] (the BKO theory with suppressed boundary conditions) the pure solvent susceptibility (the frequency-dependent Pekar factor) is evaluated as

$$[F(\omega)]^{-1}=\frac{1}{4\pi}\left(\frac{1}{\varepsilon_\infty}-\frac{1}{\varepsilon(\omega)}\right), \tag{5.3}$$

where $\varepsilon(\omega)$ is a complex-valued permittivity function of a pure solvent. This function is a counterpart of the response function $E(\omega)$ for the case of the simple continuum model. For a one-mode Debye function $\varepsilon(\omega)$ it comprises of the same single-mode function corresponding to a relaxation time equal to the longitudinal time period. It should be noted, that the phemenological description of $\varepsilon(\omega)$ used in the present study (with a high-frequency tail decaying as $1/\omega$) breaks down at high frequencies[58,59] ($\omega>10^{12}$ s.$^{-1}$), which is why we have not considered the correlation function for times faster than 1 ps.

A. Calculation of $E(\omega)$ in a Debye solvent

We took acetonitrile as a typical Debye solvent.[60] Polarity and relaxation parameters for pure acetonitrile are given in Table I. A Cole-Cole plot for $E(\omega)$ is shown in Fig. 1. It is drawn in a normalized coordinate frame $(E_2(\omega)/\Delta, E_1(\omega)/\Delta)$, where $\Delta=E(\omega=0)$. A similar plot

This article is copyrighted as indicated in the article. Reuse of AIP content is subject to the terms at: http://scitation.aip.org/termsconditions. Downloaded to IP: 134.115.2.116 On: Fri, 17 Jul 2015 07:43:17

TABLE I. Parameters of solvent polarity (static dielectric constant ε_0, high frequency constant ε_∞) and relaxation (the Debye relaxation times τ_{D_i}, the weight factors g_i) for acetonitrile[60] and dimetilformamide.[60]

	Acetonitrile[a]	Dimethylformamide
ε_0	37.84	37.25
ε_∞	3.51	2.84
τ_{D1}, s	3.37×10^{-12}	0.74×10^{-12}
τ_{D2}, s		1.036×10^{-11}
h_1	1.0	0.046
h_2		0.954

[a]Acetonitrile has a single-mode Debye spectrum, so index ''1'' is omitted in the text.

for the pure solvent (acetonitrile) susceptibility, see Eq. (5.3), is also given for the sake of comparison. Its comparison with $E(\omega)$ calculated as described in Appendix B estimates the importance of the refined theory. An accurate allowance made for the BKO boundary conditions in terms of Eqs. (4.1)–(4.10) results in more than a 20% change in $E_2(\omega)$ (as compared to the imaginary part of Eq. (5.3)) in the region where this quantity has a maximum. This implies that the one-mode Debye model is not successful in treating dynamical boundary effects in a Debye solvent. In Fig. 2 we compare the calculated function $E_2(\omega)$ with its Debye counterpart with an effective relaxation time τ_0. (The τ_0 value was defined as $\tau_0=\omega_0^{-1}$, where ω_0 is the maximum of $E_2(\omega)$). The result is $\tau_0=4.00\times10^{-13}$ s. which is compared to the experimental value of the longitudinal time period $\tau_L=3.30\times10^{-12}$ s. for acetonitrile, see Table I. The dispersion region of the calculated function is narrower than its Debye counterpart. The symmetrical shape of the Cole-Cole plot for the calculated function and the asymptotic behavior of its imaginary part imply that the Cole-Cole[61] or Davidson-Cole[62] models of dielectric dispersion are not successful in treating dynamical boundary effects in a Debye solvent.

A good approximation for the calculated function $E(\omega)$ is found in terms of a multi-mode Debye model

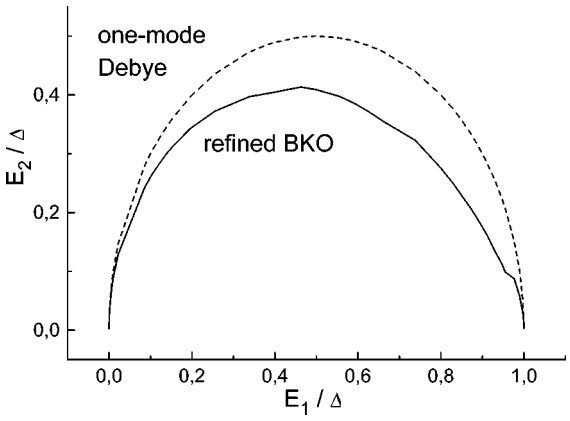

FIG. 1. Cole-Cole plot of generalized susceptibility $E(\omega)$ ($\Delta=E(\omega=0)$) for refined BKO calculations in acetonitrile. The dashed curve corresponds to the best one-mode Debye description.

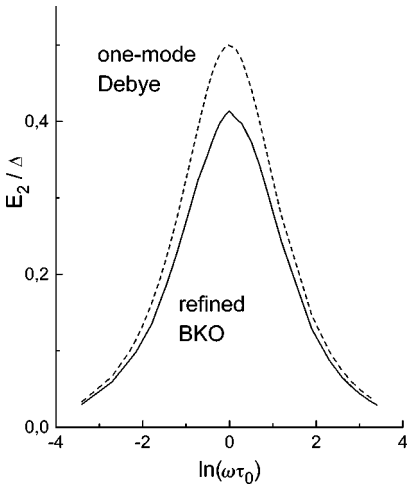

FIG. 2. Normalized plot of the imaginary part of $E_2(\omega)$, for refined BKO calculations in acetonitrile. The dashed curve corresponds to the best one-mode Debye description. τ_0 is an effective relaxation time, see the text.

$$E(\omega)/\Delta=\sum_i^n \left[\frac{g_i}{(1-i\omega\tau_i)}\right]; \quad \sum_i g_i=1, \tag{5.4}$$

where for this case $n=2$. Values of the parameters are given in Table II.

Our calculations of the TCF $C(t)$ function (see Appendix A) for the benzophenone anion in acetonitrile yield

$$C(t)=\sum_i^n g_i \exp\left(-\frac{t}{\tau_i}\right), \tag{5.5}$$

where $n=2$, i.e., $C(t)$ is fitted well by a biexponential expression. The use of Eq. (5.5) provides an illuminating format with which to discuss the results; this procedure is also commonly used to analyze time dependent fluorescence Stokes shifts data.[2,3,60] Representative results exposed in this manner are given in Table II, for the solvation of a benzophenone anion in acetonitrile. Comparison of the improved BKO data with the longitudinal relaxation time τ_L of pure acetonitrile (see Table II) reveals several interesting features. Most importantly, the biexponential fit typically yields one relaxation time slower than τ_L, with the other component faster than τ_L. In other words, inclusion of the bound-

TABLE II. Parameters of Eq. (5.4) for response function $E(\omega)$ obtained for the solvation of a benzophenone anion in acetonitrile and in dimethylformamide by the refined BKO and simple continuum calculations.

	Acetonitrile		Dimethylformamide	
	Refined BKO	Simple continuum	Refined BKO	Simple continuum
$-\Delta$, kJ/mol	77	77	95	95
τ_1, s	3.0×10^{-13}	3.3×10^{-13}	3.3×10^{-13}	3.75×10^{-13}
τ_2, s	7.4×10^{-13}		1.4×10^{-12}	1.57×10^{-12}
τ_3, s			3.5×10^{-11}	
g_1	0.72	1.0	0.50	0.68
g_2	0.28		0.45	0.32
g_3			0.05	

This article is copyrighted as indicated in the article. Reuse of AIP content is subject to the terms at: http://scitation.aip.org/termsconditions. Downloaded to IP: 134.115.2.116 On: Fri, 17 Jul 2015 07:43:17

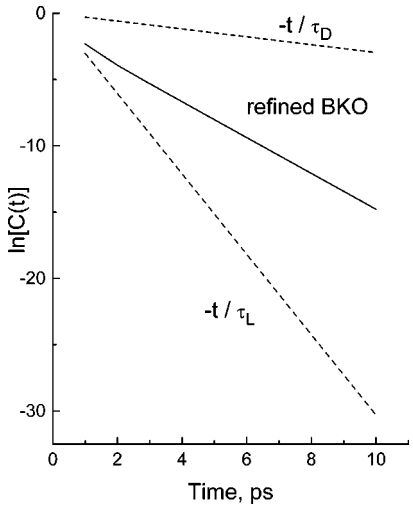

FIG. 3. The log of the TCF, $\ln[C(t)]$, plotted as a function of time for the solvation of a benzophenone anion in acetonitrile. The solid refined BKO curve is compared with two monoexponential decay laws governed by relaxation times τ_L and τ_D.

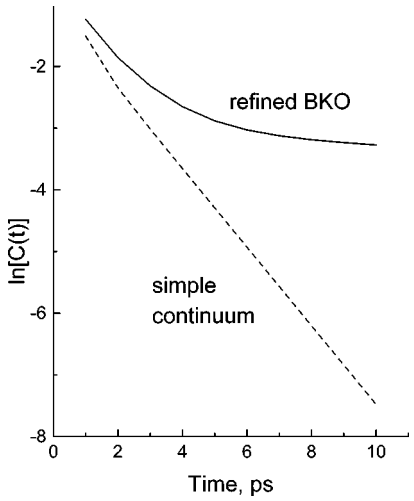

FIG. 4. The log of the TCF, $\ln[C(t)]$, plotted as a function of time for the solvation of a benzophenone anion in dimethylformamide. The solid refined BKO curve is compared with the dashed simple continuum curve.

ary conditions in the BKO theory, yields an additional relaxation component having slower dynamics than expected from the simple continuum model. Our calculations of $C(t)$ function for model anions in a Debye solvent, see Section VI B, show that the biexponential expression of $C(t)$ is quite a general result. Moreover, the following inequality holds:

$$\tau_1 < \tau_L < \tau_2 . \tag{5.6}$$

This result is well known[4–6,27] and agrees with the available experimental data, e.g., see Table 3 in Ref. 60.

In Fig. 3, $\ln[C(t)]$ is plotted for a benzophenone anion in acetonitrile. For comparison, $-t/\tau_L$ is also plotted, as well as $-t/\tau_D$, where τ_D is the Debye relaxation time of acetonitrile. It is clear that the function $C(t)$ is not well approximated by $-t/\tau_L$ but falls between the curves corresponding to the two limiting relaxation times.[6]

Taking into account Eq. (5.6), one can come to the conclusion that such a behavior of the correlation function is quite common for the ion solvation in the Debye solvents. Biexponential behavior of $C(t)$ has been found earlier with simplified cavity models, both ellipsoidal[35,63] and a combination of two cubic cells.[34] Because spatial dispersion was also disregarded in these studies, they may be considered as approximations to the present BKO scheme which treats exactly the cavity effect.

B. Calculations of $E(\omega)$ in non-Debye solvents

We took dimethylformamide as a typical non-Debye solvent. It is described by the two-mode Debye model of dielectric dispersion, see Table 3 in Ref. 60. The parameters for dimethylformamide are listed in Table I. For pure dimethylformamide a simple continuum theory predicts a two-mode Debye susceptibility function with two relaxation times τ_1 and τ_2. They are obtained by substituting the corresponding two-mode $\varepsilon(\omega)$ in Eq. (5.3) and given in Table II.

The calculation of $E(\omega)$ using the refined BKO theory yields a three-mode Debye model for benzophenone anion, see Eq. (5.4). Values of the outcome parameters are given in Table II. In our calculations the time dependence of the solvation energy is represented in terms of the TCF $C(t)$, see Eq. (5.5), where $n=3$. In Fig. 4, $\ln[C(t)]$, is plotted for a benzophenone anion in dimethylformamide. The deviation of this calculated curve from the TCF $C(t)$ obtained using the simple continuum theory (Eq. (5.3), where $\varepsilon(\omega)$ contains two Debye components) clearly demonstrates the role of the boundary conditions. This type of behavior for $C(t)$, evaluated using the refined BKO theory, is typical for non-Debye solvents, see Fig. 10a in Ref. 2.

We also studied acetone and *n*-butanol, as examples of typical non-Debye solvents described by the Cole-Cole and Cole-Davidson models of dielectric dispersion, respectively, see Table 3 in Ref. 60. In contrast to the experimental data,[60] the refined BKO theory gives for these solvents an $E(\omega)$ function, which is reasonably well approximated by the Cole-Cole and Cole-Davidson models, respectively. Probably, this result shows the restrictions of the BKO treatment, which does not take into account the ''effect of solvent structure.''

VI. ELECTRON TRANSFER PROCESSES

A. Adiabatic theory

In the simplest version, ET kinetics are determined by the evolution of the transfer charge density

$$\rho_{00} = \rho_{22} - \rho_{11} , \tag{6.1}$$

where $\rho_{22}(r)$ and $\rho_{11}(r)$ are the diagonal elements of the charge density matrix for the reactant (index ''11'') and product (index ''22'') CI states. The corresponding response function

$$[T_{in}(\omega)]_{00,00} = \lambda(\omega) = \lambda_1(\omega) + i\lambda_2(\omega) \tag{6.2}$$

This article is copyrighted as indicated in the article. Reuse of AIP content is subject to the terms at: http://scitation.aip.org/termsconditions. Downloaded to IP: 134.115.2.116 On: Fri, 17 Jul 2015 07:43:17

enters the adiabatic equation of motion for the ET medium variable

$$X=\int d^3r\rho_{00}\Phi_{in}. \tag{6.3}$$

In general, the free energy surface of an ET process, as a function of the inertial medium coordinates $Y_{ab}\equiv(Y_{in})_{ab}$, is written as[39]

$$U(Y_{ab})=-\frac{1}{2}\sum_{ab,a'b'}(T_0^{-1})_{ab,a'b'}Y_{ab}Y_{a'b'}+W_0(Y_{ab}). \tag{6.4}$$

The first term represents the self-energy associated with medium coordinates in which

$$T_0=T_{0in}=T_{in}(\omega=0) \tag{6.5}$$

is the inertial component of the static reorganization matrix (the sign has been changed as compared to the notation of Ref. 39). The second term, namely, the lowest eigenvalue of the corresponding CI Hamiltonian, represents the solute self-energy plus the solute-solvent interaction. The stochastic equation of motion for the medium coordinates reads

$$-F_0\cdot[T_{in}(\omega)]^{-1}|Y(\omega)\rangle\rangle=-|\frac{\partial W_0}{\partial Y}\rangle\rangle_\omega+|GRF\rangle\rangle \tag{6.6}$$

$$F_0^{-1}=\frac{1}{4\pi}\left(\frac{1}{\varepsilon_\infty}-\frac{1}{\varepsilon_0}\right).$$

Here we introduced the Fourier transforms $(-\partial W_0/\partial Y_{ab})_\omega$ of forces $(-\partial W_0/\partial Y_{ab})$ and collected them in a column-vector $(-|\partial W_0/\partial Y\rangle\rangle_\omega)$; the $|GRF\rangle\rangle$ indicates the vector of Fourier transformed Gaussian random forces and F_0^{-1} is the Pekar factor. This is the Fourier-transformed version of the dynamical equation obtained earlier.[37–39] Its appearance, in the context of the present linear response formulation, is very transparent. We must choose the expansion coefficients m_{ab} as

$$m_{ab}(t)=\frac{1}{F_0}\frac{\partial W_0}{\partial Y_{ab}}, \tag{6.7}$$

$$m_{ab}(\omega)=\frac{1}{F_0}\left(\frac{\partial W_0}{\partial Y_{ab}}\right)_\omega$$

and rewrite the linear response relation (3.16) as

$$|Y(\omega)\rangle\rangle=F_0^{-1}\cdot T_{in}(\omega)\cdot|\frac{\partial W_0}{\partial Y}\rangle_\omega. \tag{6.8}$$

Equation (6.6) is then found by inverting Eq. (6.8) and adding random forces in order to make allowance for fluctuations.[52]

In earlier applications this equation of motion was simplified by factorizing the reorganization matrix as

$$T_{in}(\omega)=\frac{F_0}{F(\omega)}\cdot T_0, \tag{6.9}$$

where $F(\omega)$ is given by Eq. (5.3). Here we shall abstain from this approximation. Thus, for a single variable X (6.3) we obtain the equation of motion

$$-F_0\cdot[\lambda(\omega)]^{-1}=-\left(\frac{dW_0}{dX}\right)_\omega+GRF \tag{6.10}$$

which acquires a typical form for a generalized Langevin equation (GLE)

$$[f(\omega)-f_0]X=-\left(\frac{\partial U}{\partial X}\right)_\omega+GRF \tag{6.11}$$

after introducing the following notations:

$$-F_0\cdot[\lambda(\omega)]^{-1}=f(\omega);\quad f(\omega=0)=f_0, \tag{6.12}$$

$$U(X)=\frac{f_0}{2}\cdot X^2+W_0(X).$$

Here $U(X)$ represents the ET potential profile as calculated by the CI/BO method,[39,44] with force constants $-\beta^{\neq}$ and β_0

$$\frac{dU}{dX}=-\beta^{\neq}\cdot(X-X^{\neq})(\text{at the barrier top } X=X^{\neq}), \tag{6.13}$$

$$\frac{dU}{dX}=\beta_0\cdot(X-X_0)(\text{at reactant minimum } X=X_0).$$

Finally, the Arrhenius rate prefactor of the KGH theory is

$$A=\frac{\Omega^{\neq}}{2\pi}\sqrt{\frac{\beta_0}{\beta^{\neq}}}, \tag{6.14}$$

where $\Omega^{\neq}$ is the decay frequency. As described previously,[64] it is readily expressed in terms of $\lambda(\omega)$. Thereby, the present continuum treatment, aimed at a direct evaluation of permittivity $\lambda(\omega)$, happens to be closely related to the following evaluation of the ET rate in terms of the KGH theory.

B. Calculations

We used again here only the BKO approach. The spherically symmetrical approximation for a solute needed in the nonlocal theory is hardly acceptable for studying ET. We considered ET in model anion-biradicals $(CH_2)_n^-$, where $n=4$, 6 and 8.[43,44] The geometries were taken to be the same as those of Refs. 43, 44. The CI/BO procedure was performed under the PM3 method.[44] We took a model Debye solvent (a prototype of acetone[2]), which is characterized by the following parameters: $\varepsilon_0=20.7$, $\varepsilon_\infty=1.9$ and $\tau_D=3.20\times10^{-12}$ s.

A good approximation for the calculated function $\lambda(\omega)/\Delta_1$ is found in terms of a two-mode Debye model, see Eq. (5.4), where $\Delta_1=\lambda(\omega=0)$, with $g_1=0.8$, $g_2=0.2$, $\tau_1=3.80\times10^{-13}$ s, $\tau_2=1.60\times10^{-13}$ s.

The respective changes in the ET kinetics can be visualized by considering the decay frequency $\Omega^{\neq}$ in the KGH theory as a root of the characteristic equation (see the designations in Eqs. (6.11), (6.12))

$$f(i\omega)=f_0+\beta^{\neq}. \tag{6.15}$$

This article is copyrighted as indicated in the article. Reuse of AIP content is subject to the terms at: http://scitation.aip.org/termsconditions. Downloaded to IP: 134.115.2.116 On: Fri, 17 Jul 2015 07:43:17

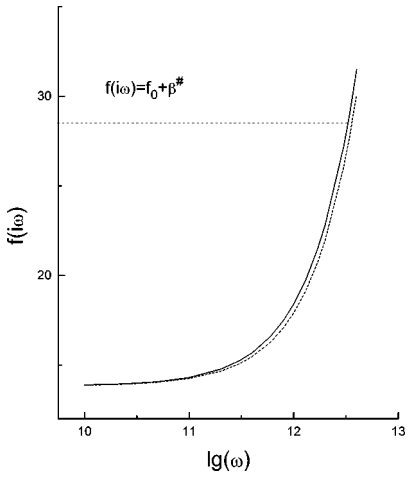

FIG. 5. Solution of the characteristic equation (6.15) for the decay frequency $\Omega^{\neq}$ for two alternatives of the function $\lambda(\omega)$, see the text, for a $(CH_2)_6^-$ model anion-biradical. The dashed curve corresponds to the simple continuum theory and the solid curve corresponds to the refined BKO theory. Here $-\beta^{\neq}$ represents a force constant at the top of the barrier of the ET potential profile, see Eq. (6.13).

As a consequence of causality,[56] $f(i\omega)$ (with real ω) is always real. Because the inverse quantity $\lambda(\omega)$ vanishes when $|\omega|\to\infty$, it can readily be evaluated on the imaginary ω axis in terms of a general relation of dispersion theory[56]

$$\lambda(i\omega)=\frac{2}{\pi}\int_0^{\infty}\frac{x\lambda_2(\omega)}{\omega^2+x^2}dx. \tag{6.16}$$

We finally obtain $f(i\omega)$ as the inverse of Eq. (6.16), according to Eq. (6.12).

The solution to Eq. (6.15) is found graphically as the abscissa of the point where the curve $f(i\omega)$ crosses the horizontal line $f(i\Omega^{\neq})=f_0+\beta^{\neq}$, see Fig. 5. This solution is unique because the causality condition ensures that $f(i\omega)$ increases monotonically.

The value of $\Omega^{\neq}$ was evaluated using for $\lambda(\omega)$ first of all a one-mode Debye model with the τ_L value, evaluated using the parameters of the model Debye solvent, and secondly a two-mode Debye model with the g_1, g_2, τ_1 and τ_2 values listed above for function $\lambda(\omega)/\Delta_1$. The first pure Debye case corresponds to the approximation (6.9) with $F(\omega)$ given by Eq. (5.3). The results are listed in Table III. The relative difference between the two $\Omega^{\neq}$ values for the first two model anion-biradicals does not exceed 13%. A strong increase in the decay frequency for $(CH_2)_8^-$ is the result of a small coupling matrix element for this case, which can be estimated from the energy gap $\Delta U^{\neq}$ (the splitting of adiabatic levels at the barrier top) as minus $\Delta U^{\neq}/2$. The potential $U(X)$ then acquires a cusp form. Strictly speaking, the corresponding kinetics must then be treated by a quantum non-adiabatic theory in which the quantity $\Omega^{\neq}$ loses its importance.

The discussion of the present Section is entirely illustrative for several reasons. First, the anions considered are purely theoretical models and there is no experimental data for them. Second, as recent studies have shown,[44] the energy profiles obtained from the simple BKO treatment give a poor description of ET energetics and must be refined by a proper account of the molecular structure of the solvent in the first solvation shell. Finally, the application of data from Table III for treating ET kinetics is consistent only for $(CH_2)_6^-$. For the case of $(CH_2)_4^-$ the barrier is too low and a steady state kinetic regime is unlikely, whereas for $(CH_2)_8^-$ a nonadiabatic ET theory must be applied.

What our computations demonstrate is how important exact boundary conditions are in treating ET kinetics. The answer is that their effect is less remarkable than in the case of time-dependent solvation spectroscopy, in agreement with the results of earlier MD computations.[17]

VII. DISCUSSION

The results of Sections V and VI show that the essential features of the solvation dynamics of ions are reasonably well reproduced in the framework of continuum medium theoretical models. Starting with a simple Debye description of a polar solvent we were able to recover a polyexponential kinetic evolution as its dynamical outcome. Our observations are complemented by the results of an approximate nonlocal theory as applied to model two-sphere charge distribution.[26] Main conclusions following from these two different approaches are in a qualitative agreement. Both the boundary effect (obtained in terms of the present BKO computation) and the effect of solvent molecular structure (a nonlocal computation, Ref. 26 and our unpublished data) only multiply a number of Debye modes involved in the resulting kinetics and shift their relaxation parameters. A relative importance of the two effects is unclear now. This ambiguity could be resolved only within a more sophisticated unique calculation, combining a nonlocal treatment with a realistic nonspherical cavity for a solute. A general structure of such a theory is outlined in Sections III, IV.

Being a first step, the present work needs further refinement in future. Two features of actual TCFs seem to be missing in our computations: oscillations and short-time

TABLE III. The decay frequency $\Omega^{\neq}$ and Arrhenius rate prefactor A of the KGH theory evaluated using one-mode (1D) and two-mode (2D) Debye models for three anion-biradicals, see the text.

	$U^{\neq}$,[a] eV	$\Delta U^{\neq}$,[b] eV	$\Omega^{\neq}$ (1D), s^{-1}	$\Omega^{\neq}$ (2D), s^{-1}	A (1D), s^{-1}	A (2D), s^{-1}
$(CH_2)_4^-$	0.16	0.51	3.67×10^{11}	3.23×10^{11}	4.20×10^{10}	3.70×10^{10}
$(CH_2)_6^-$	0.45	0.12	3.41×10^{12}	3.12×10^{12}	1.44×10^{11}	1.32×10^{11}
$(CH_2)_8^-$	0.58	0.028	1.16×10^{13}	1.10×10^{13}	2.70×10^{11}	2.56×10^{11}

[a]$U^{\neq}$ is the barrier height of the ET reaction.
[b]$\Delta U^{\neq}$ is the splitting between adiabatic levels at the barrier top.

This article is copyrighted as indicated in the article. Reuse of AIP content is subject to the terms at: http://scitation.aip.org/termsconditions. Downloaded to IP: 134.115.2.116 On: Fri, 17 Jul 2015 07:43:17

Gaussian behavior.[13,14,17,20,27] The both effects could be naturally introduced without changing the essence of our approach. Proper modifications must be brought into an input susceptibility function (such as $\varepsilon(\omega)$ in Section V A or $\chi(k,\omega)$ in Section V B). The change will be transferred to the outcome response functions and reproduce the desired temporal effects in their inverse Fourier transforms. Oscillations are expected to appear by adding resonance mode components[65] which may be either of a conventional Lorentzian form[66,67] or Gaussian.[68,65] For doing this consistently more information on the details of both the input susceptibilities and the outcome TCFs is necessary. Borrowing such information either from experiment or from MD simulations the resulting oscillatory behavior of TCFs could be generated without problems.

More vague is the problem of Gaussian initial kinetics. We displayed the results of the present calculations in terms of Lorentzian-type ω-dependencies vanishing according to an inverse power law when $|\omega|\to\infty$. In the time domain they generate exponentially decaying functions. In order to get a Gaussian component of the time evolution[13,14,17,27] one must change the Lorentzian tails of at least some of the spectral bands for Gaussian ones.[68,65] Again, if this is performed with an input susceptibility function, the result of modifying its asymptotic behavior will be transferred to the outcome response function. In the time domain this is sufficient to generate the short time component of decay kinetics. As follows from Eqs. (A4a), (A6) of Appendix A, a Gaussian tail in the imaginary part of the response function generates Gaussian short-time kinetics. Here, however, we arrive at an intrinsic deficiency in the continuum approach. The exponentially decaying high frequency portions of complex-valued response functions are not available, within a reasonable accuracy, in terms of the computational procedure described in Appendix B. This is why we report in the present article only the results obtained with Lorentzian susceptibilities.

The importance of high-frequency spectral components in steady state KGH kinetics can be also discussed. As seen from the graphical solution for the decay frequency in Fig. 5, it critically depends on the value of $f_0+\beta^{\neq}$, which determines the frequency range essential for finding $\Omega^{\neq}$. So, in Fig. 5 this region lies around $\Omega^{\neq}$ and the frequency range $\omega\gg\Omega^{\neq}$ is negligible. (Note also, that when working with frequencies $\omega>10^{13}\ \mathrm{s}^{-1}$, quantum dynamical effects become important and the whole treatment needs a deep modification). When $\Omega^{\neq}$ lies in the classical region the refinements of dynamical calculations which we introduced have little influence on the calculated rate constant.

VIII. CONCLUSIONS

In the present work we generalized a conventional SCRF approach[36] for treating polar solvation effects for computations with a complex-valued dielectric permittivity function $\varepsilon(\omega)$. This extends the idea[23,52] that, due to the properties of Maxwell's equations, a description of nonequilibrium dynamical phenomena can be gained (within a continuum theory) by simply substituting $\varepsilon(\omega)$ for the static permittivity ε_0 in static equilibrium equations. In this way calculations of TCFs were performed for complicated chemical solutes accounting for electrostatic boundary conditions and with an explicit treatment of the solute electronic structure at a reasonable quantum-chemical level.

We have formulated two methods for transforming the complex-valued SCRF results into TCFs. The first one (Sections IV, V) represents the nonstationary kinetics of the time-dependent Stokes shift and the second one (Section VI) describes the stationary monoexponential kinetics of an ET process. Although the computations were confined to the framework of the local electrostatic BKO model, their extention to a nonlocal electrostatic methodology is straightforward.

Altogether we conclude that the dynamical version of the continuum theory developed here reproduces well the low and intermediate frequency range of response functions and the corresponding intermediate and long time solvation kinetics in a nonstationary regime. Technical problems with the high-frequency range and corresponding short time kinetics seem to reflect a principal deficiency of the continuum approach. Because the opposite is true as regards the MD computations of TCFs,[13,17,69] the continuum and molecular approaches may be considered in this sense to be mutually complementary.

ACKNOWLEDGMENTS

The authors would like to thank the Russian Foundation for Fundamental Research (Project No. 96-03-32544) for providing the funding for this work. This material is based upon work supported by the U.S. Civilian Research and Development Foundation under Award No. RC1-202.

APPENDIX A: TIME CORRELATION FUNCTIONS

The TCF describing a time-resolved Stokes shift is defined as[1–7]

$$C(t)=\frac{U_S(t)-U_S(\infty)}{U_S(0)-U_S(\infty)}. \tag{A1}$$

According to formulas (4.8) and (5.1),

$$C(t)=\frac{\int_0^t E(\tau)d\tau-\Delta}{-\Delta},\quad \Delta=E(\omega=0)<0. \tag{A2}$$

Here $E(\tau)$ is the inverse Fourier transform of $E(\omega)$, Eq. (5.1). It can be expressed in terms of either $E_2(\omega)$ or $E_1(\omega)$ with the aid of the Kramers-Kronig relations. The result is[65]

$$E(\tau)=\begin{cases}\dfrac{1}{\pi}\displaystyle\int_{-\infty}^{\infty}d\omega E_1(\omega)\cos\,\omega\tau & (\tau>0)\\ \dfrac{1}{\pi}\displaystyle\int_{-\infty}^{\infty}d\omega E_2(\omega)\sin\,\omega\tau & (\tau>0)\\ 0 & (\tau<0)\end{cases}. \tag{A3}$$

Let us introduce the function $G(t)$ (where $t>0$)

This article is copyrighted as indicated in the article. Reuse of AIP content is subject to the terms at: http://scitation.aip.org/termsconditions. Downloaded to IP: 134.115.2.116 On: Fri, 17 Jul 2015 07:43:17

$$G(t)=\int_0^t E(\tau)d\tau=\frac{1}{\pi}\int_{-\infty}^{\infty}d\omega\,\frac{\sin\,\omega t}{\omega}E_1(\omega), \tag{A4a}$$

$$=-\frac{1}{\pi}\int_{-\infty}^{\infty}d\omega\,\frac{\cos\,\omega t-1}{\omega}E_2(\omega). \tag{A4b}$$

By studying the limit $t\to\infty$ we find the following relations:

$$\lim_{t\to\infty} G(t)=\Delta, \tag{A5a}$$

$$\frac{1}{\pi}\int_{-\infty}^{\infty}\frac{E_2(\omega)}{\omega}d\omega=\Delta, \tag{A5b}$$

$$\lim_{t\to\infty}\frac{1}{\pi}\int_{-\infty}^{\infty}\frac{\cos\,\omega t}{\omega}d\omega=0. \tag{A5c}$$

Expression (A5a) immediately follows from (A4a), expression (A5b) results from Eq. (6.16) when λ is changed for E_2 and $\omega=0$, and expression (A5c) follows from (A4b), (A5a) and (A5b). With this notation

$$C(t)=\frac{G(t)-\Delta}{-\Delta}. \tag{A6}$$

Let us now consider the TCF

$$J(t)=\langle Y(t)Y(0)\rangle. \tag{A7}$$

Its Fourier transform $J(\omega)$ is determined by the FDT.[56] In the high temperature limit

$$J(\omega)=\frac{2kT}{\omega}E_2(\omega). \tag{A8}$$

The inverse Fourier transform is performed with the aid of Eqs. (A5a–c). This results in the expression

$$\frac{J(t)}{\Delta}=kTC(|t|), \tag{A9}$$

and, as noted previously,[8,13,17] functions $C(t)$ and $J(t)$ are closely related.

APPENDIX B: COMPLEX-VALUED EQUATIONS FOR SURFACE CHARGE DENSITY $\sigma(r)$

The integral equation for the static BKO model reads[37]

$$\sigma(r)=\kappa_0\{[\hat{V}\rho](r)+[(\hat{S}+2\pi)\sigma](r)\}(r\in S). \tag{B1}$$

Here κ_0 is the Born factor

$$\kappa_0=\frac{1}{4\pi}\left(1-\frac{1}{\varepsilon_0}\right). \tag{B2}$$

The volume ($\hat{V}$) and surface ($\hat{S}$) integral operators need not be specified here, except to note that they are linear and their kernels are real quantities. As stated in Section IV, we now substitute for κ_0 the complex-valued permittivity

$$\kappa(\omega)=\frac{1}{4\pi}\left(1-\frac{1}{\varepsilon(\omega)}\right)=\kappa_1(\omega)+i\kappa_2(\omega) \tag{B3}$$

with

$$\kappa_1(\omega)=\frac{1}{4\pi}\left[1-\frac{\varepsilon_1(\omega)}{(\varepsilon_1(\omega))^2+(\varepsilon_2(\omega))^2}\right],$$

$$\kappa_2(\omega)=\frac{1}{4\pi}\,\frac{\varepsilon_2(\omega)}{(\varepsilon_1(\omega))^2+(\varepsilon_2(\omega))^2}. \tag{B4}$$

We anticipate that σ also becomes complex-valued

$$\sigma(\omega)=\sigma_1(\omega)+i\sigma_2(\omega) \tag{B5}$$

(the r-dependency is suppressed in the present notation for brevity). Performing the substitution $\kappa_0\to\kappa(\omega)$ and taking σ in the form (B5) in Eq. (B1), we separate the real and imaginary parts and ultimately arrive at the pair of equations

$$\sigma_1(\omega)=\kappa_1(\omega)[\hat{V}\rho(r)+(\hat{S}+2\pi)\sigma_1(\omega)]-\kappa_2(\omega)(\hat{S}+2\pi)\sigma_2(\omega),$$

$$\sigma_2(\omega)=\kappa_2(\omega)[\hat{V}\rho(r)+(\hat{S}+2\pi)\sigma_1(\omega)]+\kappa_1(\omega)(\hat{S}+2\pi)\sigma_2(\omega). \tag{B6}$$

For a first approximation, we fix $\sigma_1(\omega)$ in the first equation, and then $\sigma_2(\omega)$ in the second. Each of these equations can then be solved by standard techniques.[36] After this we may simultaneously solve the system (B6) by iterations.

[1] M. Maroncelli, J. MacInnis, and G. R. Fleming, Science **243**, 1674 (1989).
[2] M. Maroncelli, J. Mol. Liquids **57**, 1 (1993).
[3] P. F. Barbara and W. Jarzeba, Adv. Photochem. **15**, 1 (1990).
[4] B. Bagchi, Annu. Rev. Phys. Chem. **40**, 115 (1989).
[5] B. Bagchi and A. Chandra, Adv. Chem. Phys. **80**, 1 (1991).
[6] J. D. Simon, Acc. Chem. Res. **21**, 128 (1988).
[7] G. van der Zwan and J. T. Hynes, J. Phys. Chem. **89**, 4181 (1985).
[8] M. Maroncelli and G. R. Fleming, J. Chem. Phys. **89**, 5044 (1988).
[9] J. S. Bader and D. Chandler, Chem. Phys. Lett. **157**, 501 (1989).
[10] M. Maroncelli, J. Chem. Phys. **94**, 2084 (1991).
[11] R. M. Levy, D. B. Kitchen, J. T. Blair, and K. J. Krogh-Jespersen, J. Phys. Chem. **94**, 4470 (1990).
[12] T. Fonseca and B. M. Ladanyi, J. Phys. Chem. **95**, 2116 (1991).
[13] E. A. Carter and J. T. Hynes, J. Chem. Phys. **94**, 5961 (1991).
[14] M. Bruehl and J. T. Hynes, J. Phys. Chem. **96**, 4068 (1992).
[15] L. Perera and M. Berkowitz, J. Chem. Phys. **96**, 3092 (1992).
[16] E. Neria and A. Nitzan, J. Chem. Phys. **96**, 5433 (1992).
[17] B. B. Smith, A. Staib, and J. T. Hynes, Chem. Phys. **176**, 521 (1993).
[18] J. S. Bader, C. M. Cortis, and B. J. Berne, J. Chem. Phys. **104**, 2373 (1996).
[19] F. O. Raineri, Y. Zhou, H. L. Friedman, and G. Stell, Chem. Phys. **152**, 201 (1991).
[20] F. O. Raineri, H. Resat, B.-C. Perng, F. Hirata, and H. L. Friedman, J. Chem. Phys. **100**, 1477 (1994).
[21] F. O. Raineri, B.-C. Perng, and H. L. Friedman, Chem. Phys. **183**, 187 (1994).
[22] F. O. Raineri and H. L. Friedman, J. Chem. Phys. **101**, 6111 (1994).
[23] P. G. Wolynes, J. Chem. Phys. **86**, 5133 (1987).
[24] I. Rips, J. Klafter, and J. Jortner, J. Chem. Phys. **88**, 4288 (1988).
[25] I. Rips, J. Klafter, and J. Jortner, J. Phys. Chem. **94**, 8557 (1990).
[26] A. A. Kornyshev, A. M. Kuznetsov, D. K Phelps, and M. J. Weaver, J. Chem. Phys. **91**, 7159 (1989).
[27] I. Rips, in *Ultrafast Reaction Dynamics and Solvent Effects*, edited by Y. Gauduel and P. J. Rossky (AIP, New York, 1994), p. 334.
[28] B. Bagchi and A. Chandra, J. Chem. Phys. **90**, 7338 (1989).
[29] B. Bagchi and A. Chandra, J. Chem. Phys. **91**, 2594 (1989).
[30] A. Chandra and B. Bagchi, J. Phys. Chem. **93**, 6696 (1989).
[31] B. Bagchi and A. Chandra, J. Chem. Phys. **97**, 5126 (1992).
[32] A. Chandra and B. Bagchi, J. Chem. Phys. **99**, 553 (1993).
[33] L. E. Fried and M. Mukamel, J. Chem. Phys. **93**, 932 (1990).

This article is copyrighted as indicated in the article. Reuse of AIP content is subject to the terms at: http://scitation.aip.org/termsconditions. Downloaded to IP: 134.115.2.116 On: Fri, 17 Jul 2015 07:43:17

[34] X. Song, D. Chandler, and R. A. Marcus, J. Phys. Chem. **100**, 11954 (1996).
[35] C. P. Hsu, X. Song, and R. A. Marcus, J. Phys. Chem. B **101**, 2546 (1997).
[36] J. Tomasi and M. Persico, Chem. Rev. **94**, 2027 (1994).
[37] M. V. Basilevsky and G. E. Chudinov, Chem. Phys. **157**, 327 (1991).
[38] M. V. Basilevsky and G. E. Chudinov, J. Mol. Struct. (Theochem) **260**, 223 (1992).
[39] M. V. Basilevsky, G. E. Chudinov, and M. D. Newton, Chem. Phys. **179**, 263 (1994).
[40] R. Bianco and J. T. Hynes, J. Chem. Phys. **102**, 7864 (1995).
[41] M. V. Basilevsky, G. E. Chudinov, and D. V. Napolov, J. Phys. Chem. **97**, 3270 (1993).
[42] M. F. Ruis-Lopez, D. Rinaldi, and J. Bertran, J. Chem. Phys. **103**, 9249 (1995).
[43] Y.-P. Liu and M. D. Newton, J. Phys. Chem. **99**, 12382 (1995).
[44] M. V. Basilevsky, G. E. Chudinov, I. V. Rostov, Y-P. Liu, and M. D. Newton, J. Mol. Struct. (Theochem) **371**, 191 (1996).
[45] A. A. Kornyshev, in *The Chemical Physics of Solvation*, edited by R. R. Dogonadze, E. Kalman, A. A. Kornyshev, and J. Ulstrup (Elsevier, Amsterdam, 1985), p. 77.
[46] R. R. Dogonadze and T. A. Marsagishvili, in *The Chemical Physics of Solvation*, edited by R. R. Dogonadze, E. Kalman, A. A. Kornyshev, and J. Ulstrup (Elsevier, Amsterdam, 1985), p. 39.
[47] M. A. Vorotynzev and A. A. Kornyshev, *Electrostatics of a Medium with the Spatial Dispersion*, 2nd ed. (Nauka, Moscow, 1993).
[48] R. R. Dogonadze and A. A. Kornyshev, J. Chem. Soc. Faraday Trans. 2 **70**, 1121 (1974).
[49] A. A. Kornyshev, A. I. Rubinshtein, and M. A. Vorotyntsev, J. Phys. C **11**, 3307 (1978).
[50] M. A. Vorotyntsev, J. Phys. C **11**, 3323 (1978).
[51] M. V. Basilevsky and D. F. Parsons, J. Chem. Phys. **105**, 9734 (1996).
[52] M. V. Basilevsky and G. E. Chudinov, Mol. Phys. **65**, 1121 (1988).
[53] P. Hanggi, P. Talkner, and M. Borkovec, Rev. Mod. Phys. **62**, 251 (1990).
[54] Z. Xujia and C. D. Jonah, Chem. Phys. Lett. **245**, 421 (1995).
[55] Y. Lin and C. D. Jonah, J. Phys. Chem. **97**, 295 (1993).
[56] L. D. Landau and E. M. Lifshits, *Statistical Physics*, 3rd ed. (Nauka, Moscow, 1976).
[57] M. Sparpaglione and S. Mukamel, J. Chem. Phys. **88**, 3263 (1988).
[58] C. J. F. Boettcher and P. Bordewijk, *Theory of Electric Polarization*, 2nd ed. (Elsevier, Amsterdam, 1978), Vol. 2.
[59] B. Bagchi, D. W. Oxtoby, and G. R. Fleming, Chem. Phys. **86**, 257 (1984).
[60] M. L. Hong, J. A. Gardecki, A. Papazyan, and M. Maroncelli, J. Phys. Chem. **99**, 17311 (1995).
[61] K. S. Cole and R. H. Cole, J. Chem. Phys. **9**, 341 (1941).
[62] D. W. Davidson and R. H. Cole, J. Chem. Phys. **19**, 1484 (1951).
[63] E. W. Castner, G. R. Fleming, and B. Bagchi, Chem. Phys. Lett. **143**, 270 (1988).
[64] M. V. Basilevsky, A. V. Soudackov, and M. V. Vener, Chem. Phys. **200**, 87 (1995).
[65] M. V. Basilevsky and G. E. Chudinov, J. Chem. Phys. **103**, 1470 (1995).
[66] R. Kubo, M. Toda, and N. Hashitsume, *Statistical Physics II. Nonequilibrium Statistical Mechanics* (Springer-Verlag, Berlin, 1985).
[67] H. Frölich, *Theory of Dielectrics*, 2nd ed. (Clarendon Press, Oxford, 1958).
[68] I. Rips and J. Jortner, J. Chem. Phys. **87**, 2090 (1987).
[69] G. V. Vijayadamodar and A. Nitzan, J. Chem. Phys. **103**, 2169 (1995).

This article is copyrighted as indicated in the article. Reuse of AIP content is subject to the terms at: http://scitation.aip.org/termsconditions. Downloaded to IP: 134.115.2.116 On: Fri, 17 Jul 2015 07:43:17